Grenze International Journal of Engineering and Technology, Jan 2020

Studies on Al Foam Core Sandwich Composites Subjected to Flexural and Compression Loading

Sapthagiri. G[1] and Dr. H. K. Shivanand[2]
[1-2]Department of Mechanical Engg., UVCE., Bangalore University, Bangalore, Karnataka, India
Email: sapthagiri.uvce@gmail.com, shivanand.uvce@gmail.com

***Abstract*—Aluminium foam has arrange of properties that are desirable in many applications. These properties include good stiffness and strength to weight ratios, impact energy absorption, sound damping, thermal insulation and non-combustibility. Many of these characteristics are particularly attractive for core materials within sandwich structures. The combination of aluminium foam cores with thermoplastic composite skins is easily manufactured and has good potential as a multifunctional sandwich structure useful in a range of applications. This paper has investigated the flexural and Compression behaviour of such structures using an experimental technique. The development of these structures towards commercial use requires a thorough understanding of the deformation and strain mechanisms of the structure, and this will, in turn, allow predictions of their structural behaviour in a variety of loading conditions.**

***Index Terms*— Metal Foam, Carbon Fabric, Bending, Compression, Sandwich Composites.**

I. Introduction

Sandwich composite is a laminated composite specifically developed for applications requiring flexural characteristics. Developments in aviation posed the requirement of lightweight and high strength materials. Sandwich structured composites, fulfilling these requirements, became the first choice for many applications have including structural components. Now, their structural applications spread even to ground transport and marine vessels [1].

Reviewers of the history of sandwich constructions seem to disagree on who was the first person, to publish a description of the advantages of the concept of combining different materials as in a sandwich. However, the truth is probably that the idea of sandwich constructions did not come from a single person, but has occurred independently to many engineers at different times in the previous century. A few may even have recognized the principle much earlier. Fairbairn is reported to be the first person to describe the principle of sandwich constructions way back in 1849. The Mosquito fighter-bomber, built by the De Havilland Aircraft Company in England during World War II, however, is regarded as the first major application of sandwich panels [2]. The excellent performance demonstrated by this airplane instigated new research to improve techniques of fabricating sandwich structures and developing new materials to act as facings and cores. Nowadays, sandwich structures with different face sheet and core materials are increasingly used in various applications. Sandwich structures have many advantages, including high stiffness-to-weight and strength-to weight ratios, high damping capacities, good thermal insulation properties, excellent water and vapour barrier performance, good corrosion resistance, and low cost [3].

Grenze ID: 01.GIJET.6.1.1_1

The overall performance of sandwich structures depends on the material properties of the constituents (facings, adhesive and core), geometric dimensions and type of loading. Sandwich beams under general bending, shear, and in-plane loading display various failure modes. Major damage mechanisms in the composite sandwich panels in bending include, core crush, skin–core debond, core shear failure, skin delamination, and skin fracture. Failure modes and their initiation can be predicted by conducting a thorough stress analysis, and applying appropriate failure criteria in the critical regions of the beam, including three-dimensional effects [4]. This analysis is difficult because of the nonlinear and inelastic behavior of the constituent materials and the complex interactions of the failure modes. For this reason, properly designed and carefully conducted experiments are important in elucidating the physical phenomena to help the analysis.

Understanding the initiation and propagation of these damage mechanisms, therefore, imposes a tremendous challenge. A multitude of damage mechanisms could thus occur at different stages of loading, depending on the specific combinations of the parameters. Such tailoring could alter the characteristics of the load transfer between the composite skins and the core, and thereby the damage mechanisms. Especially, once the symmetry of the sandwich panels ceases to exist due to the damage initiation close to or within the loaded top skin, bending–stretching coupling could also contribute to the mechanical behavior of the panels. This strongly highlights the need for a thorough understanding of the damage initiation and propagation induced in such sandwich panels, with particular interest in the establishment of general trends of bending deformation, affected by the design parameters. This kind of experimental effort is essential to guide an effective development of future analytical engineering or numerical models for facilitating sandwich panel design.

II. Experimental Details

A. Material

Aluminium alloy were used as raw materials for manufacture of Foam Core of Sandwich Composites. The alloy nominally contains Cu: 0.7 wt.%, Mg: 1.0 wt.%, Si: 11.8 wt.%, Fe: 1.0 wt.%, Mn: 0.5 wt.%, Ni: 1.5 wt.%, Zn: 0.5 wt.%, Pb: 0.05 wt.%, Ti: 0.06 wt.%, Al: balance. The Carbon Fabric/Polypropylene prepreg was used as a Skin Material

B. Preparation of the Sandwich Specimen

Aluminium alloy Foam was made through melt foaming method by stir casting technique. Firstly, the alloy was melt at a temperature of 700-750 □. Then, preheated (1000 □ for 3 hrs) melt is Stirred by using mechanical stirring at a speed 800 rpm. stirring was continued for 2-3 minutes to ensure its complete and homogeneous mixing. Finally, dry CaH2 particles (of average size: 18μm ± 3μm at 0.6 wt.%) were added manually in the melt again through mechanical stirring. The melt temperature was varied (640 to 670 ^{o}C) to obtain varying ρ_{rd}. The temperature was maintained for another two minutes after addition of CaH_2 for complete foaming. Finally, the crucible with liquid foam cooled fast by steam spraying to get Aluminium Foam.

Materials were cut down to a size of 200 × 200 mm, with the aluminium foam cut using a band saw. The sandwich structures were made by placing a single ply of the Carbon fibre/polypropylene prepreg on either side of the aluminium foam core in a picture frame mould. Two layers of a 50μm thick hot-melt polypropylene-based adhesive were placed at each bi-material interface. This method has been found to provide good bonding between the foam and the thermoplastic skin [5].

The mould was heated to 185ºC in a heated platen press, using a thermocouple within the Twintex layer to monitor the thermoplastic temperature. The structure was then held at a pressure of 2.5 MPa while it was rapidly water cooled to consolidate the skin material. Variations in the process included altering the core thickness or using an increased number of plys of skin prepreg material. The consolidated sandwich panels with core thicknesses of 10 mm, and a single ply skin had average thicknesses of 5 mm. The apparent increase in skin thickness for the single ply skin as the core thickness increases may be related to the increase in cell diameter. During the sandwich manufacturing process the thermoplastic matrix material may experience some flow while in the liquid state before consolidation. This may result in some matrix material moving into the cells of the aluminium foam, particularly in the core with the larger cell size, reducing the overall thickness of the skin. Samples for testing were cut to width from the panels using a diamond tipped saw

C. Micrograph

To obtain optical images of specimens, a Nikon D7000 DSLR camera equipped with an AF-S VR Micro-Nikkor 105 mm f/2.8G IF-ED macro lens was used. Optical microscopy was conducted using a Nikon Epiphot 200 microscope fitted with a Nikon DS-Fil digital camera. The specimen preparation was conducted using standard metallographic procedures including grinding and polishing down to 1 μm slurry and etching using a solution of one-part nitric acid in 20 parts alcohol.

D. Static Testing

Flexural Testing

Flexural testing is conducted in a Four-point bending configuration using an Instron 4469 universal test system. Bluehill 2.0 software is used for data acquisition. The specimen orientation during bending tests is shown in Fig. 3, where the face-sheets are located at the top and bottom surfaces of the specimen and are subjected to the maximum tensile and compressive forces. At least five specimens were tested and the average values of the measured properties and their standard deviations are presented. The flexural strength (σ), flexural strain (ε_f) and the tangent modulus of elasticity (E_B) are calculated from the force–displacement curves using

$$\sigma = \frac{3FL}{2bd^2} \qquad \varepsilon_f = \frac{6Dd}{l^2} \qquad E_B = \frac{l^3 m}{4bd^3}$$

where F, b, d and l refer to load (N), specimen width (mm), specimen thickness (mm) and support span (mm) respectively. Additionally, m, and D refer to the slope of the tangent to the initial straight line portion of the force–displacement graph and maximum deflection of the centre of the beam (mm), respectively.

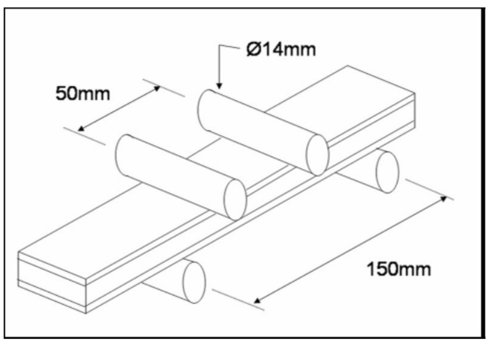

Figure 1: Four-point flexural testing geometry

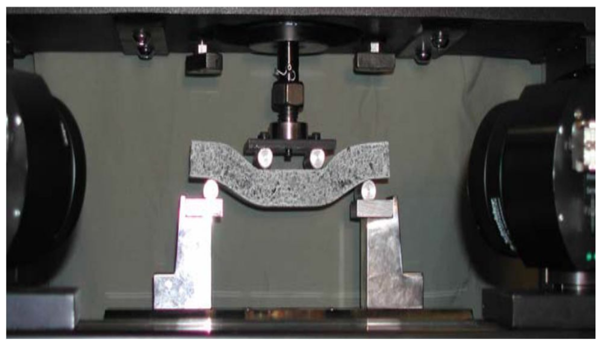
Figure 2: Image showing stereo cameras capturing four-point bend test

Compression Testing

Quasi-static compression testing was conducted using an Instron4469 universal test system, equipped with a 50kN load cell. In order to achieve the nominal initial strain rate of$10^{-3}s^{-1}$, a constant cross-head displacement rate of 0.63 mm/min was applied. The specimens used in the quasi-static compression had the dimensions of 40×40×11 mm^3. The specimens were tested in both the edgewise and flatwise orientations, where edgewise refers to having the face-sheets in the direction of the applied load and the flatwise refers to orienting the specimens with face-sheets normal to the applied load as shown in Figure 3.1. At least five specimens were tested for each orientation and the average values of measured properties as well as standard deviations are presented. Dow Corning 111 Valve Lubricant & Sealant was applied to the surfaces in contact with the compression platens to minimize friction and any barreling effects. Bluehill 2.0 software was used to acquire load and displacement data from the test system. Stress-strain graphs were developed using the load and displacement data and were used to calculate modulus, strength, failure strain and energy absorption.

III. Results

A. Flexural Test

A representative stress–strain curve obtained in the flexural testing of the syntactic foam core sandwich composite is shown in Fig. 6(a). The curve shows an initial linear elastic region. The stress drops drastically after reaching a peak. The peak corresponds to the failure of the skin on the tensile side of the specimen. Several images illustrating the failure sequence of this specimen are shown in Fig. 3(b1–b5); the locations of these observations are marked on the stress–strain graph.

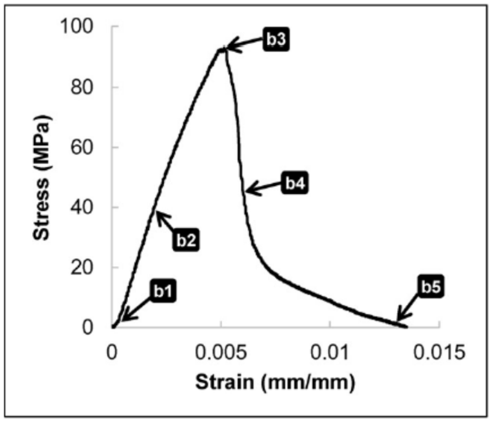

Figure 3: Representative stress–strain curve of flexural testing of a metal matrix sandwich composite

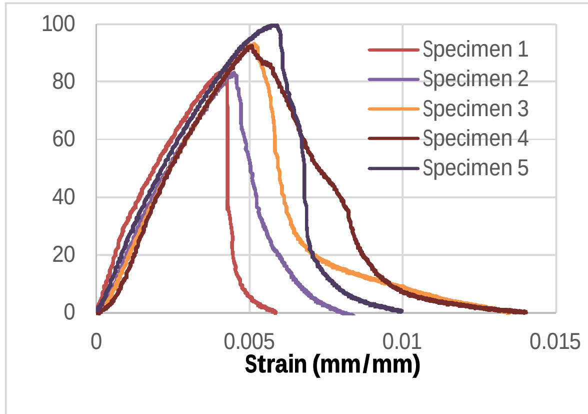

Figure-4: stress–strain curve of flexural testing of a metal matrix sandwich composite

The initial test configuration is shown in Fig. 3(b1). Fig. 3(b2) shows that there is no damage within the elastic deformation region. Fig. 3(b3) shows that at the compressive strength, the crack (marked by a circle) initiates on the tensile side of the specimen. Since the fabric is stronger than the matrix and is load bearing on the tensile side, the fabric failure leads to a transfer of load to the core, which results in rapid crack growth in the syntactic foam core. The crack growth results in stress relief in the material and reduces the load significantly (Fig. 3(b4)). Factors such as localized concentration of alumina particles and the presence of any defects in the particles or matrix close to the fabric layer contribute in determining the location of crack initiation. When the crack propagates across the core thickness (Fig. 3(b5)), the load is now transferred to the second skin. The progressive failure of the top face-sheet fabric reduces the rate of stress drop and provides additional strain before failure. Interfacial separation between core and face-sheets is not observed in this material. Interfacial failure is a common occurrence in sandwich composites under the influence of shear stresses [27]. Further tailoring of the sandwich can be conducted by Further tailoring of the sandwich can be conducted by optimizing the number of fabric layers in the skin, fabric type and core to skin thickness ratio.
The flexural strength is defined as the peak after the elastic region of the stress–strain curve and the corresponding strain is defined as the flexural strain. The modulus is calculated as the slope in the elastic region. The average flexural strength, flexural strain and modulus are measured to be 91.2 ± 5.6 MPa, 0.49 ± 0.06% and 20.06 ± 0.7 GPa respectively.

TABLE I: FLEXURAL PROPERTIES OF SANDWICH COMPOSITE

Specimen	**Max stress(MPa)**	**Flexural strain (mm/mm)**	**Modulus (GPa)**
Specimen 1	84.42	0.0040	20.1
Specimen 2	85.92	0.0045	20.1
Specimen 3	93.10	0.0051	20.9
Specimen 4	92.61	0.0051	21.8
Specimen 5	100.02	0.0058	20.2
Average	**91.2 ± 5.6**	**0.49 ± 0.06**	**20.06 ± 0.7**

Flexural strength is defined as the peak after the elastic region of the stress–strain curve and the flexural strain is defined as the strain at which the flexural strength is obtained. The modulus is calculated as the slope in the elastic region. The results are presented in Table I.

B. Compression Test

Figure 5. compares the stress-strain curve for one representative specimen of flatwise and edgewise testing of the sandwich composite. The stress-strain curves show features similar to those previously reported for metal matrix syntactic foams [6, 7, 8]. In both edgewise and flatwise cases, the stress increases nearly linearly to a

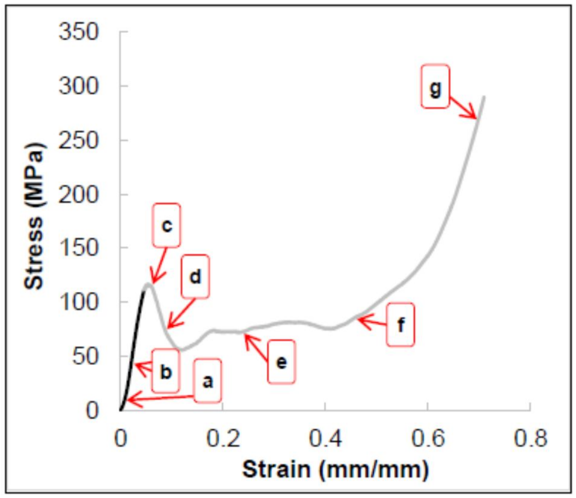

Figure 5: Representative stress–strain curve of compressive testing of a metal matrix sandwich composite

peak and then decreases before showing a stress plateau region. The plateau region reflects compression and densification of the porous foam material. At the end of the densification region, the stress starts to rise again as the fully dense material is compressed further.

Table II summarizes the average properties obtained from the quasi-static compression for specimens tested in both orientations. The compressive strength refers to the peak at the end of the elastic region. The yield strength is defined at 0.2% strain. The plateau stress is defined as the average value of stress in the region after the stress drops in the plastic region. Finally, the densification strain is defined as the value of the strain at the intersection of tangents drawn in the plateau and densification regions of the stress-strain cur

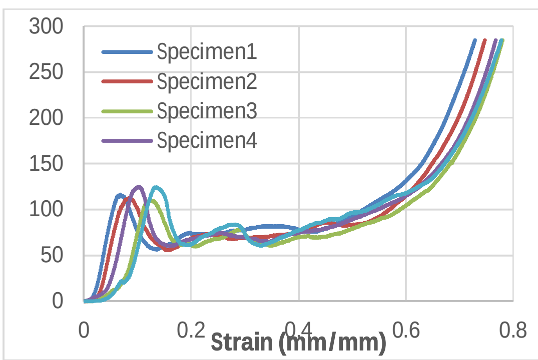

Figure-6: stress–strain curve of Flatwise Compression testing of a metal matrix sandwich composite

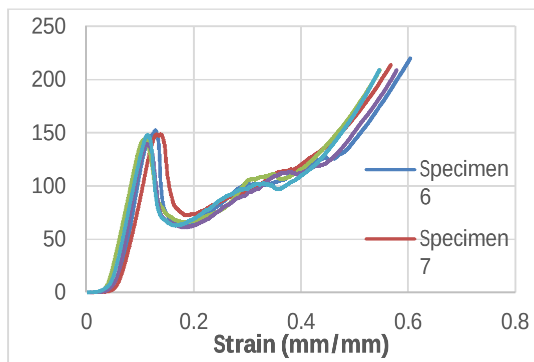

Figure-7: stress–strain curve of Flatwise Compression testing of a metal matrix sandwich composite

It is observed in Table 2 that the edgewise compressive modulus is 22% higher than the flatwise value. However, the compressive strength of the flatwise condition is observed to be 18% higher. The yield strength and plateau stress are also higher for the flatwise condition. The face-sheets are directly loaded in the edgewise orientation, which results in high modulus of the specimens. Observations of the specimen deformation pattern can help in understanding the reduction in strength in edgewise condition. Figure 5.5 and Figure 5 capture the specimen failure pattern in edgewise compression condition. The core is in front of the camera in Figure 6, whereas a face-sheet is in view in Figure 5.6. These images are taken on two different specimens but the failure sequence is found to be similar on specimens tested under the same orientation.

Fig. 8(a) shows an optical micrograph and illustrates the continuous interface between the particles and the matrix. This shows good wetting between the particles and the matrix since there are no interfacial defects between closely spaced particles. The metal matrix is highlighted in Fig. 8(b) where an aluminium-rich dendritic structure can be observed surrounded by needle-like Al–Si precipitates. A356 alloy primarily contains about 7 wt.% Si in Al. The Al–Si binary phase diagram is eutectic. As observed in the microstructure, the first solidifying phase has very low Si content and the last solidifying phase has the eutectic composition, which contains about 12.6 wt.% Si. These features can be found in the microstructure.

TABLE II: COMPRESSIVE PROPERTIES OF SANDWICH COMPOSITE

Specimen	**Density (g/cm3)**	**Modulus (GPa)**	**Compressive Strength (MPa)**
Specimen1	1.59	3.04	119.30
Specimen2	1.59	2.86	114.74
Specimen3	1.55	2.64	114.12
Specimen4	1.55	2.75	126.32
Specimen5	1.54	2.62	123.39
Edgewise	**1.57 ± 0.02**	**2.78 ± 0.15**	**119.57 ± 4.76**
Specimen	**Density (g/cm^3)**	**Modulus (GPa)**	**Compressive Strength (MPa)**
Specimen6	1.56	2.44	148.86
Specimen7	1.55	2.14	140.87
Specimen8	1.59	2.16	137.88
Specimen9	1.55	2.35	135.24
Specimen10	1.57	2.28	143.70
Flatwise	**1.56 ± 0.02**	**2.27 ± 0.13**	**141.31± 4.72**

Figure-8: (a) Optical micrograph shows the matrix region between three alumina hollow particles, (b) optical micrograph showing the matrix microstructure, (c) optical micrograph showing the carbon fibers within a face-sheet and (d) higher magnification scanning electron micrograph of carbon fibers showing the clean interface between fibers and the matrix.

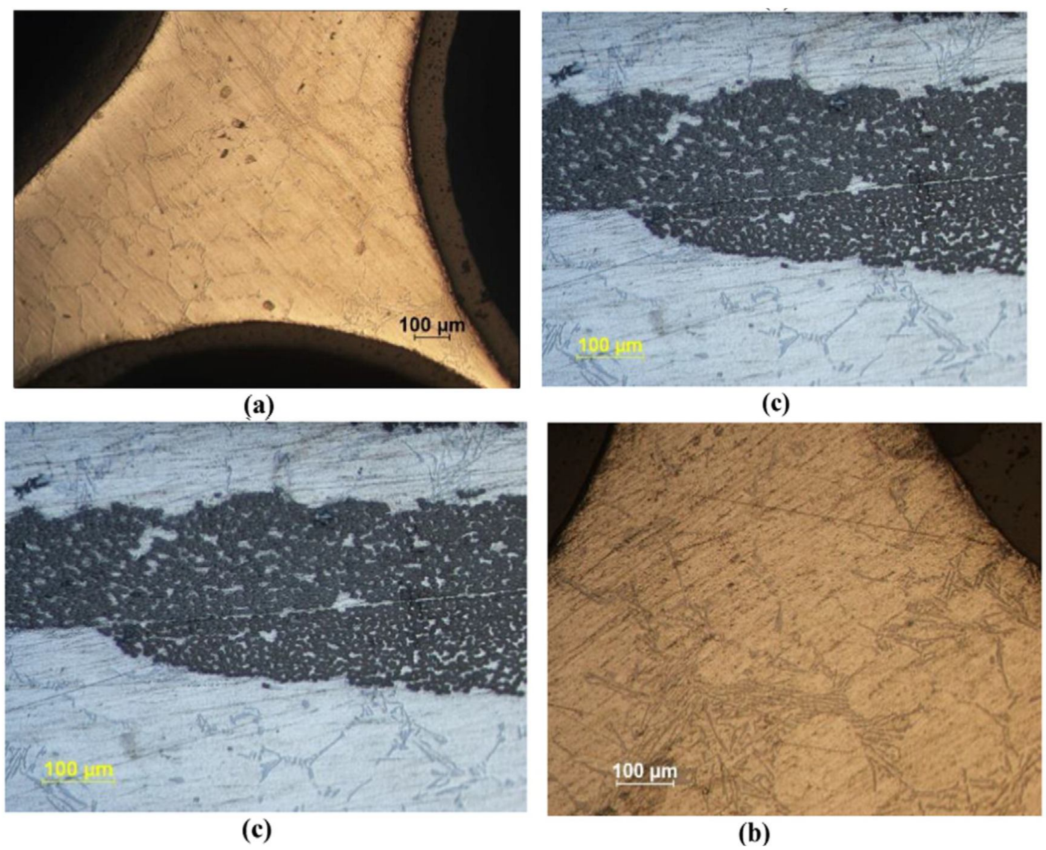

IV. CONCLUSIONS

The paper presents the fabrication of metal matrix foam core sandwich composites. The fabricated Al alloy foam core metal matrix sandwich composite contained carbon fabric reinforced face-sheets and is tested under Four-point bending conditions. The main conclusions can be summarized as follows:

- The average maximum stress, flexural strain and stiffness of the metal matrix syntactic foam core sandwich composite are measured as 91.2 ± 5.6 MPa, 0.49 ± 0.06% and 20.6 ± 0.7 GPa respectively.
- Failure mechanism indicates that the fracture is initiated in the tensile side of a specimen in three-point bending. The crack rapidly propagates to the compressive side of the specimen and ultimately leads to failure. There is no evidence of crack tip blunting or bowing, indicating strong particle–matrix interfacial bonding.
- Experimental evidence shows reasonable agreement with the calculations for sandwich composites that assumes the core and the face-sheets are monolithic and that the effect of the top sheet under compressive stress is negligible. The experimental collapse load is lower than the theoretical prediction because of the possible degradation of the face-sheets during the fabrication process.
- In the flatwise orientation, failure is dominated by the characteristics of the core material. The failure initiated by cracking of weak particles, followed by deformation of surrounding matrix due to stress transfer to the matrix after particle crushing. In the edgewise orientation, failure initiates from the carbon fabric skins. In both cases, there is shear band formation, which leads to final failure. Crushing of particles into their own voids leads to densification of the material microstructure.
- Under quasi-static conditions, the compressive strength, yield stress and plateau stress in the flatwise orientation is higher than the edgewise orientation. Furthermore, the compressive strength and yield stress of the sandwich omposite are higher than those of the core alone. This indicates the carbon fabrics have a reinforcing effect.
- Under quasi-static conditions, the sandwich composite performs better than the other syntactic foams previously reported in the literature.

REFERENCES

[1] Callister, W.D. “Materials Science and Engineering”, an Introduction. New York: John Wiley and Sons, 1997.

[2] Zenkert, D. “An Introduction to Sandwich Construction”. UK: Emas Publishing; p.111,1995.

[3] Davies, G.A.O., Hitchings, D., Besant, T., Clarke, A. and Morgan, C. “Compression after Impact Strength of Composite Sandwich Panels”. Composite Structures, Vol. 63, pp 1–9, 2004.

[4] Stephen, R., Swanson and Jongman Kim, “Failure Modes and Optimization of Sandwich Structures for Load Resistance”, Journal of Composite Materials, Vol. 37, pp. 649-667, 2003.

[5] N. Gupta, E. Woldesenbet, Characterization of flexural properties of syntactic foam core sandwich composites and effect of density variation, J. Compos. Mater. 39 (24) (2005) 2197–2212.

[6] Licitra, L., D.D. Luong, O.M. Strbik III, and N. Gupta, Dynamic properties of alumina hollow particle filled aluminium alloy A356 matrix syntactic foams. Materials & Design, 2015. 66, Part B: p. 504-515.

[7] Cox, J., D.D. Luong, V.C. Shunmugasamy, N. Gupta, O.M. Strbik, and K. Cho, Dynamic and Thermal Properties of Aluminium Alloy A356/Silicon Carbide Hollow Particle Syntactic Foams. Metals, 2014. 4(4): p. 530-548.

[8] Luong, D.D., O.M. Strbik III, V.H. Hammond, N. Gupta, and K. Cho, Development of high performance lightweight aluminium alloy/SiC hollow sphere syntactic foams and compressive characterization at quasi-static and high strain rates. Journal of Alloys and Compounds, 2013. 550: p. 412-422.

[9] Ashby, M.F., A.G. Evans, N.A. Fleck, L.J. Gibson, J.W. Hutchinson, and H.N.G. Wadley, Chapter 1 - Introduction, in Metal Foams, M.F. Ashby, et al., Editors. 2000, Butterworth-Heinemann: Burlington. p. 1-5.

[10] Banhart, J., Manufacture, characterisation and application of cellular metals and metal foams. Progress in Materials Science, 2001. 46(6): p. 559-632.

[11] Gupta, N. and P.K. Rohatgi, Metal matrix syntactic foams: processing, microstructure, properties and applications2014: DEStech Publications, Inc.

[12] Orbulov, I.N. and J. Ginsztler, Compressive characteristics of metal matrix syntactic foams. Composites Part A: Applied Science and Manufacturing, 2012. 43(4): p. 553-561.

[13] Mondal, D.P., N. Jha, A. Badkul, S. Das, and R. Khedle, High temperature compressive deformation behaviour of aluminium syntactic foam. Materials Science and Engineering: A, 2012. 534: p. 521-529.

[14] Santa Maria, J.A., B.F. Schultz, J.B. Ferguson, and P.K. Rohatgi, Al–Al2O3 syntactic foams – Part I: Effect of matrix strength and hollow sphere size on the quasi-static properties of Al-A206/Al2O3 syntactic foams. Materials Science and Engineering: A, 2013. 582: p. 415-422.

[15] Ferguson, J.B., J.A. Santa Maria, B.F. Schultz, and P.K. Rohatgi, Al–Al2O3 syntactic foams—Part II: Predicting mechanical properties of metal matrix syntactic foams reinforced with ceramic spheres. Materials Science and Engineering: A, 2013. 582: p. 423-432.

[16] Zou, L.C., Q. Zhang, B.J. Pang, G.H. Wu, L.T. Jiang, and H. Su, Dynamic compressive behavior of aluminium matrix syntactic foam and its multilayer structure. Materials & Design, 2013. 45: p. 555-560.

[17] Balch, D.K., J.G. O'Dwyer, G.R. Davis, C.M. Cady, G.T. Gray III, and D.C. Dunand, Plasticity and damage in aluminium syntactic foams deformed under dynamic and quasi static conditions. Materials Science and Engineering: A, 2005. 391(1–2): p. 408-417.

[18] Hartmann, M., K. Reindel, and R. Singer. Fabrication and properties of syntactic magnesium foams, Porous and Cellular Materials for Structural Applications. In Symposium Proceeding.

[19] Luong, D.D., V.C. Shunmugasamy, N. Gupta, D. Lehmhus, J. Weise, and J. Baumeister, Quasi-static and high strain rates compressive response of iron and Invar matrix syntactic foams. Materials & Design, 2015. 66, Part B: p. 516-531.